HHS Public Access

Author manuscript

J Med Primatol. Author manuscript; available in PMC 2020 May 19.

Published in final edited form as:

J Med Primatol. 2020 February ; 49(1): 26–33. doi:10.1111/jmp.12438.

BCL6 BTB-specific Inhibition via FX1 Treatment Reduces Tfh Cells & Reverses Lymphoid Follicle Hyperplasia in Indian Rhesus Macaque (*Macaca mulatta*)

Yanhui CAI[1], **Meagan A. Watkins**[2], **Fengtian Xue**[3], **Yong Ai**[3], **Huiming Cheng**[3], **Cecily C. Midkiff**[2], **Xiaolei Wang**[2], **Xavier Alvarez**[2], **Adi Narayana Reddy Poli**[4], **Joseph M. Salvino**[4], **Ronald S. Veazey**[2], **Luis J. Montaner**[1]

[1]HIV-1 Immunopathogenesis Laboratory, The Wistar Institute, 3601 Spruce Street, Philadelphia, PA, USA 19104

[2]Division of Comparative Pathology, Tulane National Primate Research Center, 18703 Three Rivers Road, Covington, LA, USA 70433

[3]Department of Pharmaceutical Sciences, University of Maryland School of Pharmacy, Baltimore, MD, USA 21201

[4]Molecular and Cellular Oncogenesis Program, The Wistar Institute, 3601 Spruce Street, Philadelphia, PA, USA 19104.

Abstract

Background—The BTB domain of BCL6 protein was identified as a therapeutic target for B-cell lymphoma. This study compared the pharmacokinetics (PK) of the BCL6 BTB inhibitor (FX1) between mice and macaques, as well as evaluating its lymphoid suppressive effect in uninfected macaques with lymphoid hyperplasia.

Materials & Methods—Eight uninfected adult Indian rhesus macaques (*Macaca mulatta*) were used in the study, four animals carrying lymphoid tissue hyperplasia. Plasma FX1 levels were measured by HPLC-MS/MS. Lymph node biopsies were used for H&E and immunohistochemistry staining, as well as mononuclear cell isolation for flow cytometry analysis.

Results—Inhibition of the BCL6 BTB domain with FX1 led to a reduction in the frequency of GC, Tfh $CD4^+$, and Tfh precursor cells, as well as resolving lymphoid hyperplasia, in rhesus macaques.

Conclusions—BCL6 inhibition may represent a novel strategy to reduce hyperplastic lymphoid B cell follicles and decrease Tfh cells.

Correspondence: Luis J. Montaner, D.V.M., M.Sc., D.Phil., HIV-1 Immunopathogenesis Laboratory, The Wistar Institute, 3601 Spruce Street, Room 480, Philadelphia, PA 19104. montaner@wistar.org; Phone: (215) 898-3934; Fax: (215) 573-9272.

Author's contributions: Y.C. participated in the study design, data analysis/interpretation, and manuscript preparation; M.A.W. participated in the sample processing, flow staining, and data analysis; J.M.S, F.X., A. Y. and H.C. synthesized FX1, participated in the drug formulation and data interpretation; C.CM and X.A participated in the immunostaining, confocal imaging, and analysis of results; X.W. and R.S.V participated in the experimental design and data interpretation; L.J.M. participated in the study design, data interpretation, and manuscript preparation.

Conflict-of-interest disclosure: The authors declare no competing financial interest.

Keywords

BCL6; Tfh; Germinal center reaction; Lymphoid hyperplasia

Introduction

BCL6 (B-cell lymphoma 6) was identified as a therapeutic target for B-cell lymphoma and diseases associated with elevated BCL6 expression (1–4). BCL6 was initially identified as an oncogene in diffuse large B-cell lymphoma (DLBCL) due to chromosomal translocation(4, 5), and later recognized as a transcriptional repressor for some genes associated with DNA damage checkpoints and cell proliferation (4). Sequence analysis indicated that BCL6 point mutations or small deletions were observed in 70% DLBCL, 45% follicular lymphoma, 58% acquired immunodeficiency syndrome (AIDS)-related non-Hodgkin's lymphomas (NHL), and >43% of post-transplantation lymphoproliferative disorders (6).

BCL6 protein is preferentially found in the germinal center (GC) B cells and T follicular helper (Tfh) cells. BCL6 is a critical transcriptional factor for Tfh cell differentiation, and the expression of BCL6 protein is essential for the GC reaction during humoral immune responses (7–10). Abnormal regulation of BCL6 expression, e.g., hypermethylation followed by upregulation, is associated with deviated Tfh cell generation and the onset of T-cell lymphoma(11). During the development of $CD4^+$ Tfh cell, BCL6 is increased in $CD4^+$ T cells when naïve cells are primed by dendritic cells (DC), and upregulated with CXCR5 during Tfh cell migration into the GC (12). We further confirmed that the expression of BCL6 proteins in *ex vivo* anti-CD3/28 activated $CD4^+$ T cells was higher than that in naïve or resting $CD4^+$ T cells(13). Together, the expression of BCL6 protein is associated with both GC B-cell proliferation and T cell activation.

BCL6 is a tri-modular domain protein that contains an N-terminal BTB/POZ domain, a secondary repression domain, and a C-terminal DNA binding domain (4, 14). The BTB domain recruits BCL6 co-repressor proteins (e.g., SMRT, NCOR, and BCOR), mediates BCL6 dimerization (14) and regulates the germinal center formation. Recently, a novel BCL6 BTB-specific inhibitor (FX1) was identified using the Site Identification by Ligand Competitive Saturation (SILCS) approach (3, 15). FX1 binds to an aromatic pocket within the lateral groove of BTB domain (unique to BCL6 protein) with >4 folds higher affinity than its natural ligand (SMRT), and impedes BCL6 from recruiting its repressor proteins (3, 15). FX1 is not toxic and can effectively act against large B-cell lymphoma cells *ex vivo* and *in vivo* (3, 15). Blocking BCL6 BTB domain with FX1 treatment reduces T-cell dependent germinal center reaction, and limits immune activation *in vivo*(3), as well as represses HIV infection of Tfh $CD4^+$ cells *ex vivo (13)*.

This study evaluated the pharmacokinetics (PK) of FX1 in rhesus macaques and mice, and assessed the lymphoid suppressive effect of FX1 in uninfected macaques with lymphoid hyperplasia. Our study provides the basis for dosing FX1 in rhesus macaques as a preamble to preclinical studies using nonhuman primates and clinical development of targeting BCL6 BTB domain in humans.

Materials and methods

Nonhuman primates study design and sample collections

Eight uninfected adult Indian rhesus macaques (*Macaca mulatta*) aged 4~12 years old were used in the study. Four macaques were diagnosed with follicular and paracortical hyperplasia and used for the PK, tolerability and efficacy study for FX1 (provided by Dr. Fengtian XUE at the University of Maryland); four healthy macaques were used as the controls in the study. Of those 4 macaques carrying lymphoid hyperplasia, two received FX1 at 10mg/kg subcutaneously (S.Q.) in 4mL vehicle that comprised 30% propylene glycol, 65% PEG-400, 5% Dextrose (5%), the other two at 25mg/kg. Each animal was given one injection of FX1 S.Q. and underwent five blood collections (at 0, 2, 4, 6 and 24hr). After resting for twelve days, an 8-day course FX1 treatment was performed daily (except 7-day course FX1 treatment for one animal receiving FX1 at 25mg/kg). We lost the animal receiving high dose (25mg/kg) FX1 after 7 dose treatment due to cardiac arrest from complications of anesthesia but unrelated to FX1 treatment. Plasma samples were fractionated for PK analysis of FX1 level by HPLC-MS/MS (Alliance Pharm, Malvern, PA). Axillary or inguinal lymph node biopsies were collected at baseline and 48hr after last FX1 treatment for H&E and immunohistochemistry staining, as well as mononuclear cell isolation for flow cytometry analysis. All procedures with macaque animals were performed according to the “NIH Guide for the Care and Use of Laboratory Animals” and were approved by the Tulane University Institution Animal Care and Use Committee under protocol #P0371.

Mice pharmacokinetic study and sample collections

Male adult CD-1 mice received the same FX1 doses as in macaques yet in 100 μL vehicle given intraperitoneally (i.p.) as a comparator of PK between species. A total of 21 mice were used in the study. Eighteen mice received FX1 and underwent six blood collection with three mice at each time point (0.5, 2, 4, 6, 8 and 24hr later). Three mice received an equivalent volume of vehicle and underwent blood collection at 24hr later as the negative control. PK study in mice was done in the animal facility at Alliance Pharm (Malvern, PA) and approved by the IACUC approved at the Wistar Institute under protocol #112754.

Isolation of mononuclear cells from lymph node tissue

Lymph node biopsy tissues were obtained and preserved in 5 ml of RPMI1640 (Cellgro; Manassas, VA) supplemented with 5% fetal bovine serum (Gibco, cat no. 26140–079; Grand Island, NY, USA), 100 IU/ml of penicillin/streptomycin (EMD Millipore, Billerica, MA), and 2 mM of L-glutamine (Cellgro; Manassas, VA). After removal of the adipose tissue around the lymph node biopsy, single-cell suspensions from lymph node biopsy were prepared by meshing the cells through 100 μM cell strainer (BD; San Jose, USA) with a sterile 5 mL syringe plunger (BD; San Jose, USA). The cell suspensions underwent centrifugation at 2000 rpm for 10 min (Beckman, Allegra X-12R, Brea, CA, USA) and washed with 2% PBS-FBS (PBS containing 2% FBS). Two million lymph node mononuclear cells (LNMC) were used for flow staining, and the rest cells were suspended in BAMBANKER™ serum-free cell culture freezing medium (Wako Laboratory Chemicals, cat no. 302–14681; Richmond, VA) and stored in liquid nitrogen until further analyses.

Flow cytometry and data analysis

Two million of LNMC or PBMC were stained for flow cytometry as previously described to analyze the expression of surface and intracellular markers as well as cellular composition using the 3-laser FACS Fortessa (Becton Dickinson; San Jose, USA)(16). Antibodies used in these analyses were purchased from either BD or Biolegend and included anti-CD16 (clone 3G8), anti-CD11b (clone M1/70), anti-CD1c (clone L161), anti-CD8 (clone SK1), anti-CD14 (clone M5E2), anti-CD11c (clone 3.9), anti-CD4 (clone OKT4), anti-CD20 (clone 2H7), anti-CD123 (clone 7G3), anti-HLA-DR (clone Immu-357), anti-CD3 (clone SP34–2), anti-CCR6 (clone GO34E3), anti-PD1 (clone EH12.2H7), anti-CD28 (clone 28.2), anti-CD69 (clone FN50), anti-CD95 (clone DX2), anti-CDCXCR3 (clone G025H7), anti-CD25 (clone M-A251), anti-Ki67 (clone B56), anti-CXCR5 (clone 1C6), and anti-CCR7 (clone 3D12). A minimum of 100,000 $CD3^+$ T cells were collected, and post-acquisition analysis performed by Y.C. using FlowJo (Version 9.6, TreeStar) software.

Histochemical staining and histopathological evaluation of lymph node biopsy tissue

Lymph node biopsies were processed for H&E staining. Briefly, tissue was fixed in 10% neutral-buffered formalin, sectioned to 6 μm thickness, and stained with hematoxylin and eosin (H&E) using automated Leica autostainer XL (Leica Biosystems; Buffalo Grove, IL). The images of stained tissue sections were captured under regular light microscopy at 100x magnification. Baseline and end of treatment time-point lymph node tissue sections from macaques receiving FX1 were evaluated for (1) follicular hyperplasia evidenced by an increase in the amount and size of follicle caused by stimulating of B cells and abnormal proliferation of cells within the secondary lymphoid tissue follicles, and (2) paracortical hyperplasia evidenced by an increase in area of the cortex and medullar within the interfollicular stimulation of the T cells in the paracortex.

Antibody staining and confocal microscopy imaging

Lymph node biopsy tissue sections were incubated with anti-CD3 (polyclonal, #A0452; DAKO, Santa Clara, CA), anti-CD20 (clone L26, #M0755; DAKO) and Ki67 (clone MIB-1, #M7240; DAKO), or anti-CD3, anti-CD68 (#sc20060; Santa Cruz, Dallas, TX) and BCL6 (clone BCL6/1527, #ab218952; Abcam, Cambridge, UK) following the protocols as previous described (16). Imaging was performed with a Leica TCS SP2 confocal microscope equipped with three lasers (Leica Microsystems) at 200x, 400x or 630x magnification. Three to five images were collected from each lymph node tissue section. Adobe Photoshop software (Version 7.0; Adobe Systems) was used to process and assemble the images.

Results

Pharmacokinetic study of FX1 in macaques and mice

In macaques, circulating plasma FX1 levels peaked at 2hr after one administration, declined immediately, and cleared within 24hr (Fig 1); the peak plasma FX1 concentrations (C_{max}) were 155nM for the animals receiving 25mg/kg but 1/3 lower in those macaques receiving 10mg/kg (data not shown). In the CD-1 mice, C_{max} occurred at 7000nM at 0.5hr post-dosing. The half-life ($T_{1/2}$) of FX1 was 9.51hr in mice, shorter than observed in macaque

(3.37hr) (Table 1). One dose of FX1 at 25mg/kg i.p. in mice led to drug exposure level (AUC_{0-t}) of 47,300 nM×h/mL while equal dose S.Q. was 821 nM×h/mL in macaques (Table 1). An effective dose of FX1 in mice that could kill B-cell lymphoma cells *in vivo* was 100mg/kg was equivalent to 25mg/kg in macaques according to FDA conversion (17).

BCL6 BTB domain inhibition via FX1 treatment effectively reduced Tfh and Tfh precursor cells in LN of macaques

We performed flow cytometry to analyze the frequency of Tfh/Tfh precursor cells and immunofluorescence staining of the tissue sections to analyze the expression of BCL6 protein in the LN of normal macaques and those macaques with lymphoid hyperplasia at baseline (pre-treatment), as well as compare their changes after receiving the 8-day course FX1 treatment (except 7-day course FX1 treatment for one animal receiving FX1 at 25mg/kg). As expected, flow cytometry analysis indicated that LN $CXCR5^+CD4^+$ T cells were higher in the macaques with lymphoid hyperplasia than those in healthy control animals (Fig 2A & 2B). The increased $CXCR5^+CD4^+$ T cells in macaques with hyperplasia (median=26%, n=4) were restored to level observed in controls (median=16%, n=2) after FX1 treatment at 25mg/kg (Fig 2A & 2B), but did not change (median=26%, n=2) when FX1 was dosed at 10mg/kg (Fig 2A & 2B). The increased $CXCR5^+CD4^+$ T cells during hyperplasia were more significant in Tfh subset ($CXCR5^+PD1^{hi}CD4^+$; median=8%, n=2 in macaques with hyperplasia vs. median=1%, n=5 in healthy macaques, Fig 2C & 2D) but less evident in Tfh precursor cells ($CXCR5^+PD1^{dim/-}CD4^{+,}$; median=20%, n=4 in macaques with hyperplasia vs. median=18%, n=5 in healthy macaques; Fig 2C & 2E). FX1 treatment resulted in a profound loss of $BCL6^+$ Tfh (median=1.5%, n=2; Fig 2C & 2D), and Tfh precursor cells (median=15%, n=2; Fig 2C & 2E). A lowered BCL6 protein expression after FX1 was noted by immunofluorescent staining of lymph node tissue sections before and after an 7- or 8-day course treatment with FX1 at 25mg/kg for (Fig 2F).

BCL6 BTB domain inhibition via FX1 treatment effectively lowered the degree of lymphoid hyperplasia in rhesus macaques

FX1 treatment reduced GC reaction and lowered the frequency/area of GC in a T cell-dependent immunized mice model (3), we expected it would also reduce macaque lymphoid hyperplasia. We performed H&E staining to examine the lymph node architecture and immunofluorescent staining to investigate the expression of Ki67 (a cell cycle protein indicating cellular proliferation). The macaques with lymphoid hyperplasia presented with an increased frequency and size of lymphoid follicles (B cell compartment) and the area of the cortex and medullar within the interfollicular zone (rich in T cells) (Fig 3A&B) when compared to healthy macaques (Fig 3E). An 7- or 8-days course treatment with FX1 at 25mg/kg, but not 8-days course treatment with FX1 at 10mg/kg, resulted in a lower frequency of GC when compared to baseline (Fig 3C&D). Baseline Ki67 expression was abundant in the lymph node GC from the macaques with lymphoid hyperplasia (Fig 3F&G), especially in GC T cells (Fig 3J). High dose FX1 treatment, but not low dose FX1 treatment, resulted in a decrease of $Ki67^+$ B and T cells within GC (n=2) (Fig 3H&I).

BCL6 BTB domain inhibition via FX1 treatment did not cause any systemic adverse effect in rhesus macaques with lymphoid hyperplasia

We further analyzed the LMNC by flow cytometry and monitored the animals' body weight, complete blood counts (CBC) and blood chemistry at baseline and after the 8-day course FX1 treatment (Fig 4A). We lost one animal receiving high dose FX1 after 7 dose treatment due to cardiac arrest from complications of anesthesia but unrelated to FX1 treatment. No significant changes were detected in immune cell subsets in the PBMC or LMNC (Fig 4B). Although we observed a drop in the $CD4^+$ T cells in the LMNC we did not detect a change in the PBMC(Fig 4C). We interpret this to reflect a reduction in proliferating $CD4^+$ T cells associated with lymphoid hyperplasia. The animals' body weight, complete blood counts (CBC) and blood chemistry test results were maintained at the level similar to baseline during and after FX1 treatment (Fig 4D–F).

Discussion

Our study is the first time documenting that lymphoid proliferation in rhesus macaques could be reduced following inhibition of BCL6 BTB domain using small inhibitor molecular (FX1). We confirm that FX1 PK differs between mice and macaques, but dose-conversion following FDA conversion method regardless of the route of injection (17). However, we observed FX1 is lipophilic with very low aqueous solubility (1.46ng/mL in PBS) which will require improving water solubility for better biodistribution. As we observed elevation of T cell activation among all animals with no difference between the doses used, it is likely the effect could be mediated by the vehicle. It remains to be addressed if the reduced germinal center reaction due to FX1 treatment could be reversed in rhesus macaques; and if there is any long-term adverse effect, e.g., negative impact on existing humoral immunity. Data obtained from this pilot study agrees with the observation of anti-lymphoma effect from FX1-treatment in mice (3, 15), but requires to be validated with a larger amount of macaques.

We observed FX1 dosing could lower B-cell follicles and the frequency of Tfh $CD4^+$ T and Tfh precursor cells, providing a scientific premise of evaluating dosing in humans and whether this strategy can be applied to reduce Tfh cells in settings where reduction of this subset can be a therapy target such as HIV-infected ART-treated individuals. Indeed, germinal center $BCL6^+CD4^+$ Tfh are highly susceptible to HIV infection and thought to be a sanctuary site for replication-competent viral reservoir following antiretroviral therapy (ART) (18–20). Two mechanisms have been raised for the preferential retention of HIV within Tfh $CD4^+$ T cells in spite of ART: (a) limited GC tissue distribution of antiretroviral drugs (21, 22); and/or (b) limited ability of cytotoxic $CD8^+$ T cells or NK cells to enter the GC to control/eliminate HIV-infected Tfh cells due to low expression levels of the chemokine receptor CXCR5 (18, 20, 23). The difference between pathogenic SIV infection of rhesus macaque and non-pathogenic SIV infection of the natural hosts (e.g., African green monkeys) revealed the lack of viral persistence in the lymphoid GC (24, 25), and highlighted the importance of eliminating the virus from the secondary lymphoid tissues. It remains to be tested whether BCL6 BTB domain inhibition via FX1 may represent a novel

strategy to reduce the retention of SIV/HIV in Tfh reservoir in infected individuals undergoing ART.

In summary, our data support the observation of maintaining FX1 levels in plasma in association with tissue modulation in a decrease in germinal centers and Tfh cells.

Acknowledgements

We thank Aubrey Leso and James Hayden from the Wistar Imaging Shared Resouce for capturing the images from the H&E stained slides. We are grateful for the technical assistance from Dr. Marissa D Fahlberg from the flow cytometry core and Dr. Taylor M. Joshua from the Division of Veterinary Medicine at TNPRC. We are grateful for the Shared Resources Facilities at the Wistar Institute supported by a Cancer Center Support Grant (P30CA010815) and the Confocal Image Core at TNPRC supported by an S10 award (OD019964). This study was supported by The BEAT-HIV Delaney Collaboratory (UM1AI126620, co-funded by NIAID, NIMH, NINDS, and NIDA) to L.J.M., and an NHP pilot award from the UPenn CFAR to L.J.M; the additional support was provided by The Philadelphia Foundation (Robert I. Jacobs Fund), Kean Family Professorship, Ken Nimblett and the Summerhill Trust, AIDS funds from the Commonwealth of Pennsylvania and from the Commonwealth Universal Research Enhancement Program, Pennsylvania Department of Health, the Penn Center for AIDS Research (P30 AI 045008), and Wistar Cancer Center Grant (P30 CA10815). The funders had no role in study design, data collection and analysis, decision to publish, or preparation of the manuscript.

The content is solely the responsibility of the authors and does not necessarily represent the official views of the National Institutes of Health.

References

1. Cerchietti L, Melnick A. 2013 Targeting BCL6 in diffuse large B-cell lymphoma: what does this mean for the future treatment? Expert Rev Hematol 6:343–345. [PubMed: 23991920]
2. Huang F, Jin Y, Wei Y. 2016 MicroRNA-187 induces diffuse large B-cell lymphoma cell apoptosis via targeting BCL6. Oncol Lett 11:2845–2850. [PubMed: 27073562]
3. Cardenas MG, Yu W, Beguelin W, Teater MR, Geng H, Goldstein RL, Oswald E, Hatzi K, Yang SN, Cohen J, Shaknovich R, Vanommeslaeghe K, Cheng H, Liang D, Cho HJ, Abbott J, Tam W, Du W, Leonard JP, Elemento O, Cerchietti L, Cierpicki T, Xue F, MacKerell AD Jr., Melnick AM. 2016 Rationally designed BCL6 inhibitors target activated B cell diffuse large B cell lymphoma. J Clin Invest 126:3351–3362. [PubMed: 27482887]
4. Cardenas MG, Oswald E, Yu W, Xue F, MacKerell AD Jr., Melnick AM. 2017 The Expanding Role of the BCL6 Oncoprotein as a Cancer Therapeutic Target. Clin Cancer Res 23:885–893. [PubMed: 27881582]
5. Ueda C, Akasaka T, Ohno H. 2002 Non-immunoglobulin/BCL6 gene fusion in diffuse large B-cell lymphoma: prognostic implications. Leuk Lymphoma 43:1375–1381. [PubMed: 12389616]
6. Hyjek E, Chadburn A, Liu YF, Cesarman E, Knowles DM. 2001 BCL-6 protein is expressed in precursor T-cell lymphoblastic lymphoma and in prenatal and postnatal thymus. Blood 97:270–276. [PubMed: 11133771]
7. Nurieva RI, Chung Y, Martinez GJ, Yang XO, Tanaka S, Matskevitch TD, Wang YH, Dong C. 2009 Bcl6 mediates the development of T follicular helper cells. Science 325:1001–1005. [PubMed: 19628815]
8. Basso K, Dalla-Favera R. 2012 Roles of BCL6 in normal and transformed germinal center B cells. Immunol Rev 247:172–183. [PubMed: 22500840]
9. Hatzi K, Melnick A. 2014 Breaking bad in the germinal center: how deregulation of BCL6 contributes to lymphomagenesis. Trends Mol Med 20:343–352. [PubMed: 24698494]
10. Poholek AC, Hansen K, Hernandez SG, Eto D, Chandele A, Weinstein JS, Dong X, Odegard JM, Kaech SM, Dent AL, Crotty S, Craft J. 2010 In vivo regulation of Bcl6 and T follicular helper cell development. J Immunol 185:313–326. [PubMed: 20519643]
11. Nishizawa S, Sakata-Yanagimoto M, Hattori K, Muto H, Nguyen T, Izutsu K, Yoshida K, Ogawa S, Nakamura N, Chiba S. 2017 BCL6 locus is hypermethylated in angioimmunoblastic T-cell lymphoma. Int J Hematol 105:465–469. [PubMed: 27921272]

12. Baumjohann D, Okada T, Ansel KM. 2011 Cutting Edge: Distinct waves of BCL6 expression during T follicular helper cell development. J Immunol 187:2089–2092. [PubMed: 21804014]
13. Cai Y, Abdel-Mohsen M, Tomescu C, Xue F, Wu G, Howell BJ, Ai Y, Sun J, Azzoni L, Le Coz C, Romberg N, Montaner LJ. 2019 BCL6 Inhibitor-Mediated Downregulation of Phosphorylated SAMHD1 and T Cell Activation Are Associated with Decreased HIV Infection and Reactivation. J Virol 93.
14. Lin LY, Evans SE, Fairall L, Schwabe JWR, Wagner SD, Muskett FW. 2018 Backbone resonance assignment of the BCL6-BTB/POZ domain. Biomol NMR Assign 12:47–50. [PubMed: 28929458]
15. Beguelin W, Teater M, Gearhart MD, Calvo Fernandez MT, Goldstein RL, Cardenas MG, Hatzi K, Rosen M, Shen H, Corcoran CM, Hamline MY, Gascoyne RD, Levine RL, Abdel-Wahab O, Licht JD, Shaknovich R, Elemento O, Bardwell VJ, Melnick AM. 2016 EZH2 and BCL6 Cooperate to Assemble CBX8-BCOR Complex to Repress Bivalent Promoters, Mediate Germinal Center Formation and Lymphomagenesis. Cancer Cell 30:197–213. [PubMed: 27505670]
16. Hasegawa A, Liu H, Ling B, Borda JT, Alvarez X, Sugimoto C, Vinet-Oliphant H, Kim WK, Williams KC, Ribeiro RM, Lackner AA, Veazey RS, Kuroda MJ. 2009 The level of monocyte turnover predicts disease progression in the macaque model of AIDS. Blood 114:2917–2925. [PubMed: 19383966]
17. Sharma V, McNeill JH. 2009 To scale or not to scale: the principles of dose extrapolation. Br J Pharmacol 157:907–921. [PubMed: 19508398]
18. Paiardini M, Lichterfeld M. 2016 Follicular T helper cells: hotspots for HIV-1 persistence. Nat Med 22:711–712. [PubMed: 27387885]
19. Miles B, Connick E. 2016 TFH in HIV Latency and as Sources of Replication-Competent Virus. Trends Microbiol 24:338–344. [PubMed: 26947191]
20. Fukazawa Y, Lum R, Okoye AA, Park H, Matsuda K, Bae JY, Hagen SI, Shoemaker R, Deleage C, Lucero C, Morcock D, Swanson T, Legasse AW, Axthelm MK, Hesselgesser J, Geleziunas R, Hirsch VM, Edlefsen PT, Piatak M Jr., Estes JD, Lifson JD, Picker LJ. 2015 B cell follicle sanctuary permits persistent productive simian immunodeficiency virus infection in elite controllers. Nat Med 21:132–139. [PubMed: 25599132]
21. Fletcher CV, Staskus K, Wietgrefe SW, Rothenberger M, Reilly C, Chipman JG, Beilman GJ, Khoruts A, Thorkelson A, Schmidt TE, Anderson J, Perkey K, Stevenson M, Perelson AS, Douek DC, Haase AT, Schacker TW. 2014 Persistent HIV-1 replication is associated with lower antiretroviral drug concentrations in lymphatic tissues. Proc Natl Acad Sci U S A 111:2307–2312. [PubMed: 24469825]
22. Lorenzo-Redondo R, Fryer HR, Bedford T, Kim EY, Archer J, Pond SLK, Chung YS, Penugonda S, Chipman J, Fletcher CV, Schacker TW, Malim MH, Rambaut A, Haase AT, McLean AR, Wolinsky SM. 2016 Persistent HIV-1 replication maintains the tissue reservoir during therapy. Nature 530:51–56. [PubMed: 26814962]
23. Gonzalez-Figueroa P, Roco JA, Vinuesa CG. 2017 Germinal Center Lymphocyte Ratios and Successful HIV Vaccines. Trends Mol Med 23:95–97. [PubMed: 28089302]
24. Huot N, Bosinger SE, Paiardini M, Reeves RK, Muller-Trutwin M. 2018 Lymph Node Cellular and Viral Dynamics in Natural Hosts and Impact for HIV Cure Strategies. Front Immunol 9:780. [PubMed: 29725327]
25. Huot N, Jacquelin B, Garcia-Tellez T, Rascle P, Ploquin MJ, Madec Y, Reeves RK, Derreudre-Bosquet N, Muller-Trutwin M. 2017 Natural killer cells migrate into and control simian immunodeficiency virus replication in lymph node follicles in African green monkeys. Nat Med 23:1277–1286. [PubMed: 29035370]

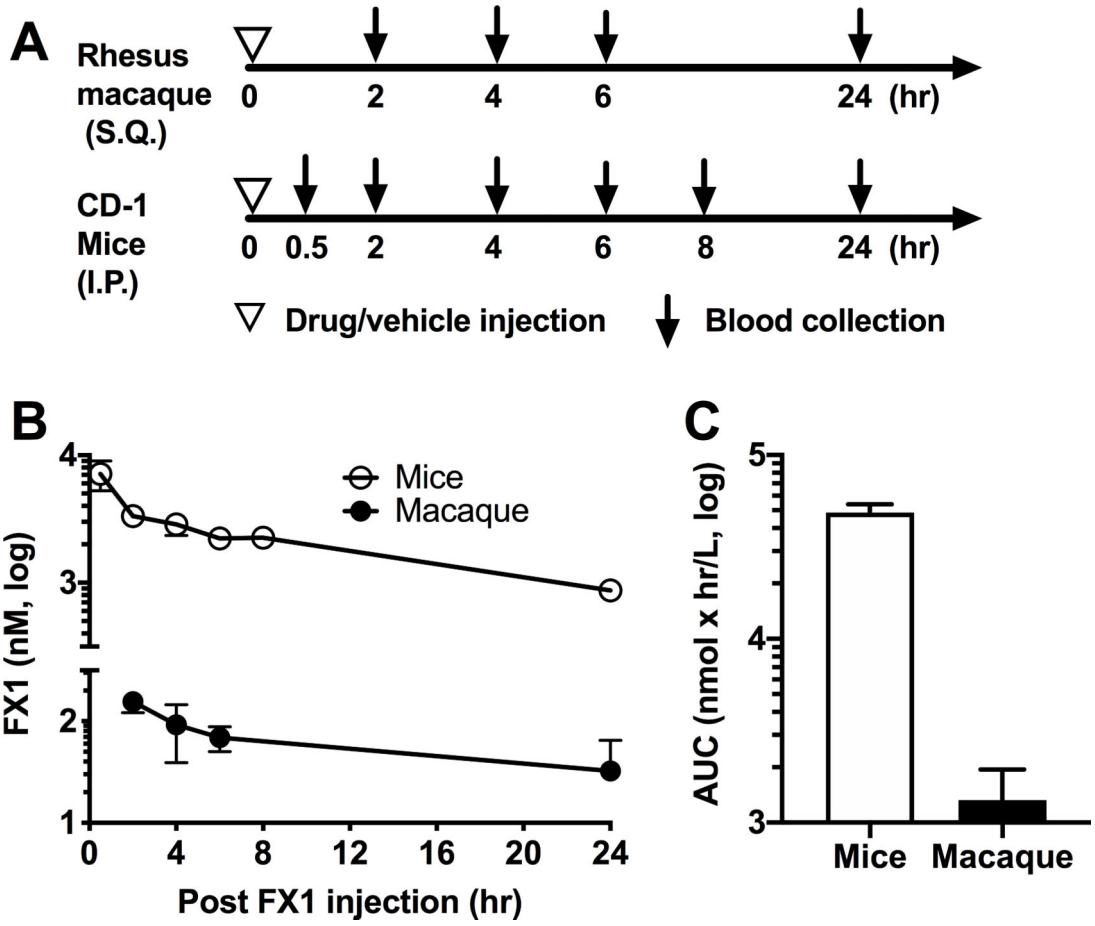

Figure 1. Pharmacokinetic of BCL6 BTB inhibitor (FX1) in uninfected rhesus macaques and mice.

(A) Schematic diagram of the experimental design. Two Indian rhesus macaques received one dose of FX1 at 25mg/kg S.Q. and then underwent five blood collection at 0, 2,4,6 and 24hr later. 18 CD-1 mice received on FX1 at 25mg/kg I.P. and then underwent six blood collections with each collection including three mice at 0.5, 2,4,6, 8 and 24hr later. Additional 3 CD-1 mice received vehicle were used for collecting blood at 24hr later as the negative control. **(B)** The plasma FX1 concentrations measured at 0, 0.5, 2, 4, 6, 8 and 24hr after one dose of FX1 injection were presented. **(C)** The FX1 exposure level in mice and macaques was calculated using the area under the curve (AUC) and presented. Mean and standard error were indicated in panel **B** and **C**.

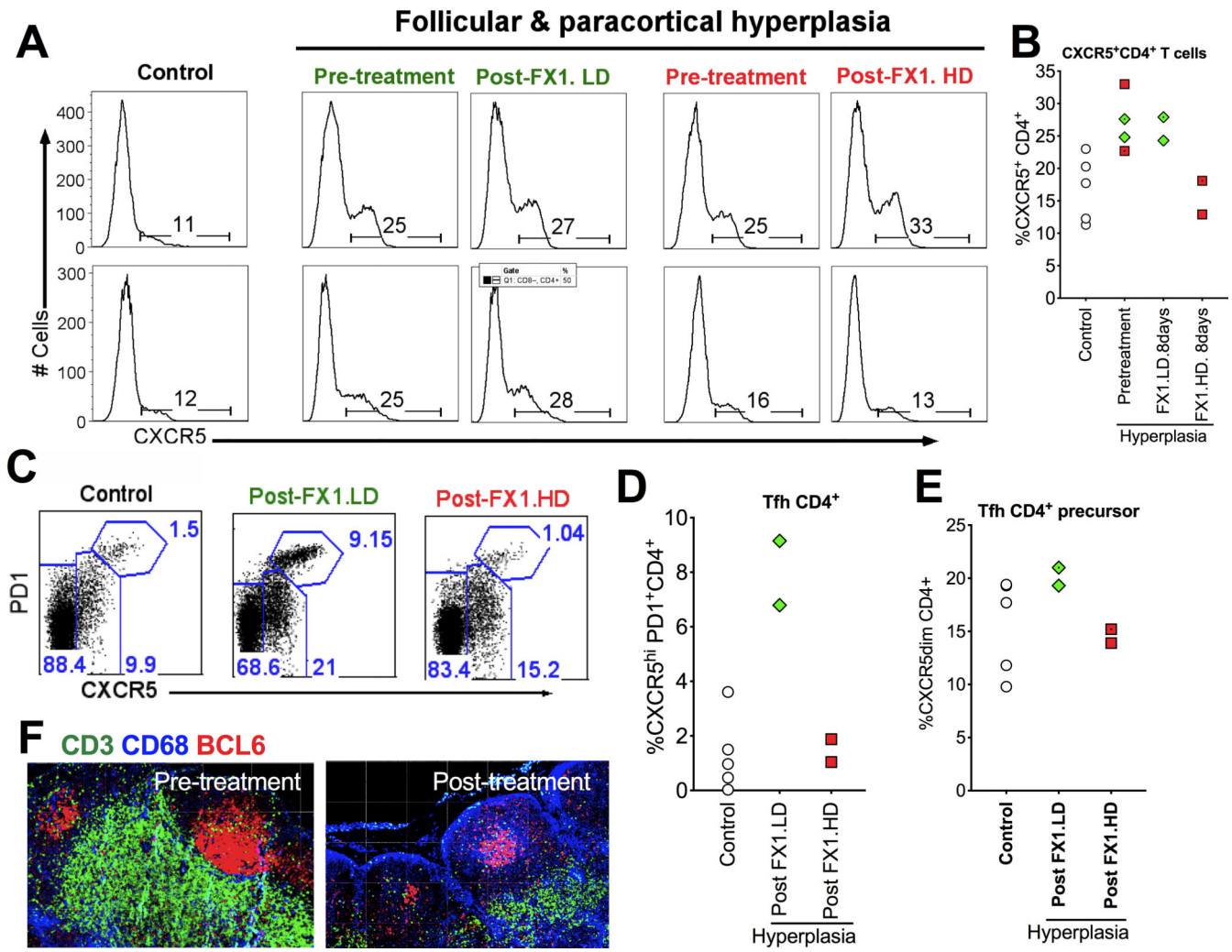

Figure 2. BCL6 BTB inhibitor (FX1) treatment reduced the frequency of lymphoid Tfh CD4$^+$ T cells and its precursor cells.

(A-B) Representative histogram **(A)** and summary **(B)** showing the frequency of CXCR5$^+$CD4$^+$ T cells in the lymph node of healthy control macaques, macaques with lymphoid hyperplasia, and those macaques with lymphoid hyperplasia receiving an 8-day course FX1 treatment (except 7-day course FX1 treatment for one animal receiving FX1 at 25mg/kg). **(C)** Representative flow plot for the frequency of CXCR5^{hi}PD1^{hi} Tfh CD4$^+$ T cells and its precursor cells (CXCR5^{dim}CD4$^+$) in the lymph node of four healthy control macaques, macaques with lymphoid hyperplasia, and those macaques with lymphoid hyperplasia receiving an 7- or 8-day course FX1 treatment at 25mg/kg. **(D-E)** The frequency of Tfh **(D)** and Tfh CD4$^+$ precursor cells **(E)** in lymph nodes from four macaques with lymphoid hyperplasia at baseline and 48hr after an 7- or 8-day course FX1 treatment, as well as four healthy control macaques. **(F)** Representative images for the lymph node biopsies from the same adult macaques with lymphoid hyperplasia before (left) and 48hr (right) after FX1 treatment (25mg/kg). Anti-CD3 (green), anti-CD68 (blue), and anti-BCL6 (red) are presented. Images were captured at 200x magnification.

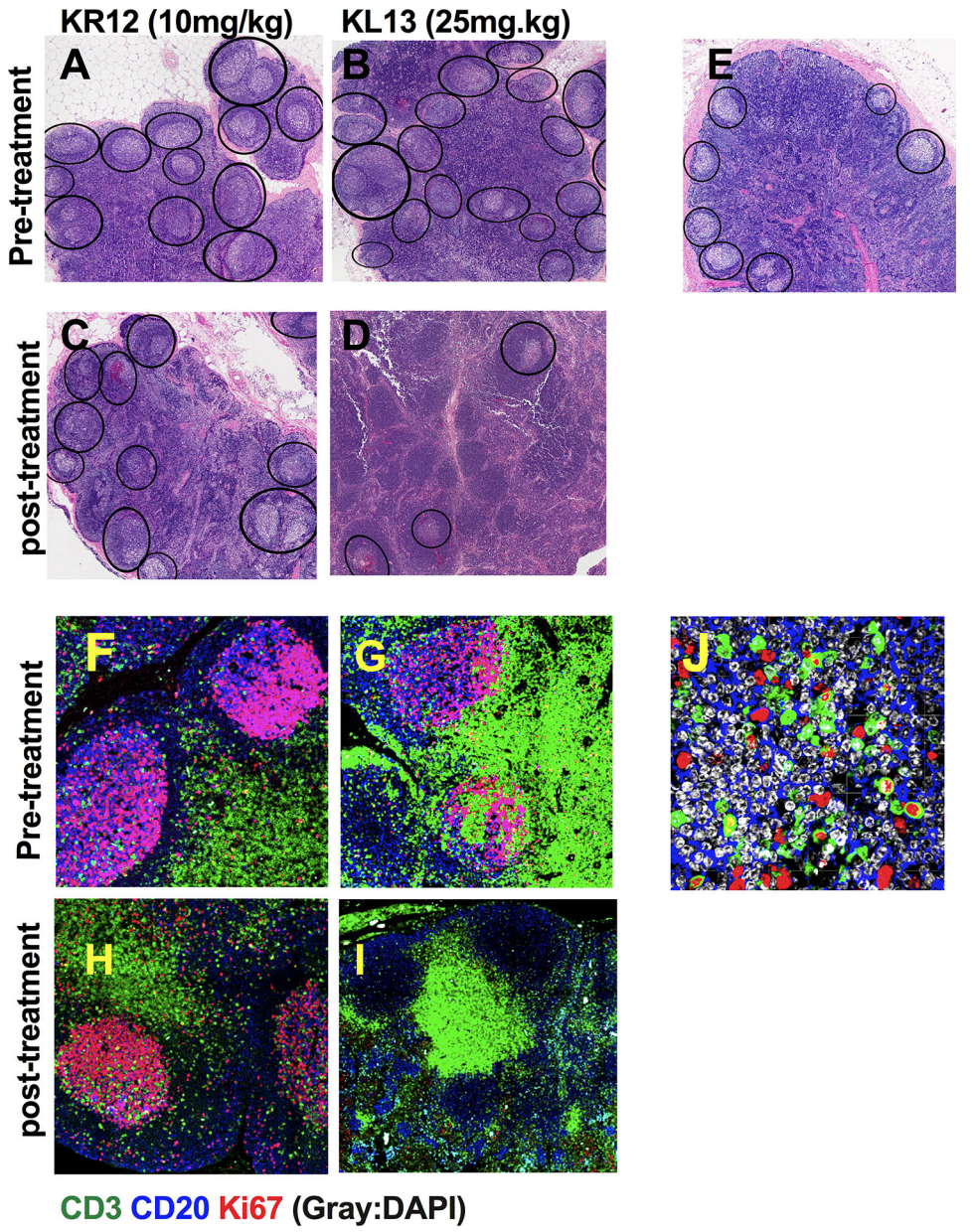

Figure 3. BCL6 BTB inhibitor (FX1) treatment reduced lymphoid hyperplasia and Ki67$^+$ T cells in the germinal center.

Lymph node biopsies were collected from four adult macaques exhibiting lymphoid hyperplasia at baseline and 48hr after an 8-day course FX1 treatment. **(A-D)** H&E staining of lymph node biopsies at baseline **(A&B)** and after **(C&D)** 10mg/kg **(C)** and 25mg/kg **(D)** FX1 treatment for an 8-day course are presented. **(E)** Representative images for H&E stained lymph node tissue sections from healthy rhesus macaques. Images were captured at 100x magnification; Germinal center areas are highlighted in each section (see black ovals). **(F-I)** Immunofluorescence staining of the lymph node biopsies from macaques with lymphoid hyperplasia before treatment (F&G) and after receiving BCL6 FX1 treatment at 10mg/kg **(H)** and 25mg/kg **(I)**. **(J)** Higher mangnification of baseline (pre-treatment) images are shown for the expression of Ki67 in the germinal center T cells. The tissue sections were

stained with anti-CD3 (green), anti-CD20 (blue), anti-Ki67 (red) and DAPI (grey). Images were captured at 400x magnification.

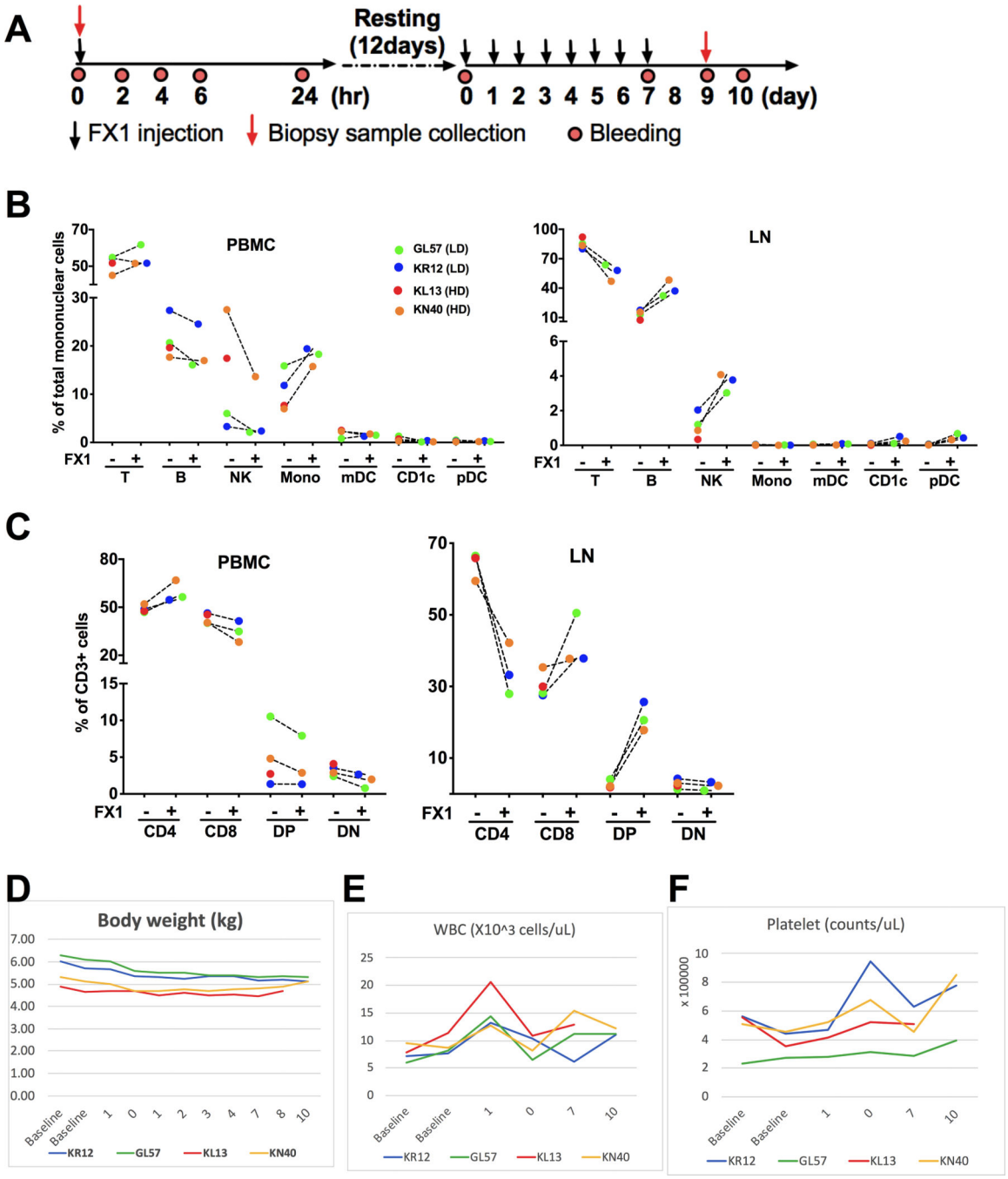

Figure 4. BCL6 BTB inhibition via FX1 treatment did not cause any systemic adverse effect in rhesus macaques with lymphoid hyperplasia.

(A) A schema for FX1 injection, blood collection, and lymph node biopsy sample collection in the study. **(B)** The frequency of immune response cells in the PBMC and lymph node were analyzed by flow cytometry and presented. **(C)** The frequency of T cell subsets [$CD4^+$, $CD8^+$, double positive (DP), double negative (DN)] in the PBMC and lymph node analyzed by flow cytometry were presented. **(D)** The body weight measured before and after FX1 treatment was presented. **(E-F)** The white blood cell counts (WBC) **(E)** and platelet **(F)**

obtained by CBC analysis were presented. Note panel B lists color code for animal data shown in panels **B-G**.

Table 1

Summary for PK studies of FX1 in mice and macaques

Drug administered	**FX1**	
Measured		
Animal species	**CD-1 mice**	**Indian Rhesus macaque**
Dose (mg/kg)	25	25
Route	I.P.	S.Q.
Parameter		
Cmax (nM/mL)	7000	155
Tmax (h)	0.5	2
T1/2 (hr)	9.51	3.37
AUC 0-t, (nM *h/mL)	47300	821.3
Mean, n/time point	3	2